Available online at www.sciencedirect.com
SCIENCE DIRECT®
Journal of Sound and Vibration 294 (2006) 381–387
JOURNAL OF SOUND AND VIBRATION
www.elsevier.com/locate/jsvi

Short Communication

Buckling loads of columns with constant volume

Byoung Koo Lee[a,*], Athol J. Carr[b], Tae Eun Lee[a], Il Jung Kim[c]

[a]*Department of Civil and Environmental Engineering, Wonkwang University, Iksan, Junbuk 570-749, Republic of Korea*
[b]*Department of Civil Engineering, University of Canterbury, Private Bag 4800, Christchurch, New Zealand*
[c]*Division of Architecture and Civil Engineering, Jeonbuk Science College, Jeongeup, Jeonbuk 580-712, Republic of Korea*

Received 26 August 2005; received in revised form 15 October 2005; accepted 7 November 2005
Available online 27 December 2005

Abstract

This paper investigates buckling loads of columns with constant volume. The parabolic and sinusoidal tapers with solid regular polygon cross-sections are adopted as the column taper. The differential equation governing the buckled shape of such column is derived and solved for calculating the buckling loads. The clamped–clamped, clamped–hinged and hinged–hinged ends constraints are considered in numerical examples. The buckling loads are presented as functions of non-dimensional system parameters. The section ratios and buckling load parameters of the strongest columns are reported.

1. Introduction

Since columns are basic structural forms, their static and dynamic behaviors have been studied extensively. In column problems, predicting the buckling loads is very important for structural design. The column behavior under load depends on the cross-sectional shape, type of taper and the volume of the column [1,2]. Predicting buckling loads of non-prismatic columns, which have the same volume with specific length, are especially attractive in the viewpoint of optimal design.

Since Lagrange attempted to determine the optimum shape for a column in 1773, many investigators have studied the mechanical behavior of beams/columns with constant volume. Keller [3], Tadjbakhsh and Keller [4], and Taylor [5] derived the shape of the strongest columns and their critical buckling loads. Here, the strongest column was defined as the elastic column of a given length and volume which can carry the highest axial load without buckling. Keller and Niordson [6] studied the tallest columns. The optimal structural design under multiple eigenvalue constraints was investigated by Masur [7]. Stability experiments on the strongest columns were conducted by Wilson et al. [8]. Barnes [9], and Cox and Overton [10] determined the shape of the strongest column. Atanackovic and Simic [11] determined the optimal shape of a simply supported column loaded by uniformly distributed follower type of load. Lee and Oh [12] investigated the elastica and buckling load of simple tapered columns with constant volume.

*Corresponding author. Tel.: +82 63 850 6718; fax: +82 63 857 7204.
E-mail addresses: bkleest@wonkwang.ac.kr (B.K. Lee), a.carr@civil.canterbury.ac.nz (A.J. Carr), telee@wonkwang.ac.kr (T.E. Lee), platepro@jbsc.ac.kr (I.J. Kim).

0022-460X/$ - see front matter
doi:10.1016/j.jsv.2005.11.004

Recent theories predict the optimal shapes for highest axial loads for columns. Although many numerical results were presented in the literature, the configurations of the columns are very limited in various aspects. For instance, circular cross-sectional shapes, linear column tapers, hinged–hinged end constraints were considered in most previous work.

The main purpose of the present paper is to investigate the buckling loads of solid tapered columns with the regular polygon cross-section and a constant volume. The differential equation governing the buckled shape of the linear elastic column is derived by using the relationship between the natural frequencies and loads in free vibration problems.

The governing equation is solved numerically by the Runge–Kutta method and determinant search method combined with the Regula–Falsi method. The parabolic and sinusoidal tapers are chosen for the tapered column. In the numerical examples, the clamped–clamped, clamped–hinged and hinged–hinged end constraints are considered.

The buckling loads are presented as functions of non-dimensional system parameters. The section ratios and buckling load parameters of the strongest columns are reported. Also, the effect of taper type on the buckling load parameter is reported.

2. Column with constant volume

Shown in Fig. 1(a) is a solid tapered column with span length l and constant volume V. The cross-sectional shape of the column is the regular polygon cross-section and its cross-sectional depth, which is varied with the coordinate x, is expressed as h. Therefore, the column has a variable area and a variable moment of inertia of area of cross-section expressed as A and I, respectively. The variation of depth h with x is defined in Fig. 1(b). The depths of both ends ($x = 0$ and l) and mid-span ($x = l/2$) are h_0 and h_m, respectively. Here, a non-dimensional parameter defined as section ratio n is defined as follows:

$$n = \frac{h_m}{h_0}. \tag{1}$$

The cross-sectional properties A and I of the regular polygon cross-section with depth h are, respectively [12],

$$A = \frac{m}{2}\sin\left(\frac{\pi}{m}\right)h^2, \quad I = \frac{m}{4}\sin\left(\frac{\pi}{m}\right)\cos^3\left(\frac{\pi}{m}\right)\left[1 + \frac{1}{3}\tan^2\left(\frac{\pi}{m}\right)\right]h^4, \tag{2,3}$$

where m is the integer number of sides of the regular polygon cross-section. It is clear that A and I converge to πh^2 and $\pi h^4/4$, respectively, as m approaches ∞, i.e. the section becomes circular. Also, it is noted that every

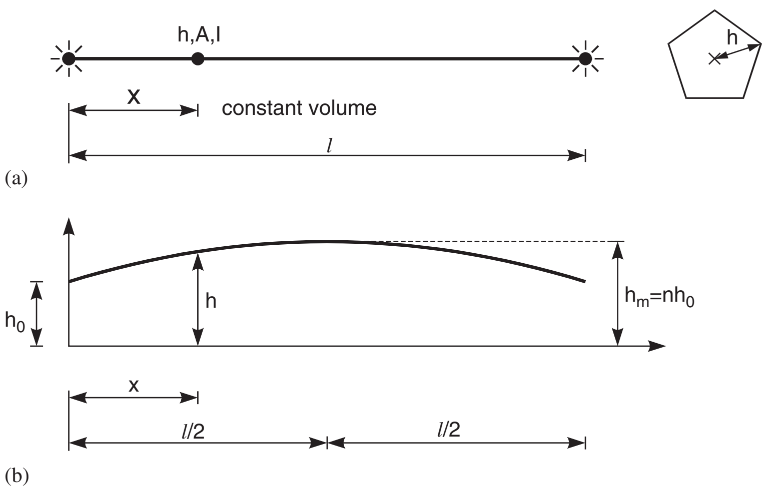

Fig. 1. Column having regular polygon cross-section with constant volume and its variable cross-sectional depth.

centroidal axis of a regular polygon cross-section is a principal axis and has the same moment of inertia, expressed by Eq. (3).

Now, define the variable cross-sectional depth h shown in Fig. 1(a) and (b). In this study, the parabolic and sinusoidal tapers are chosen for columns with variable depth h. For the parabolic taper, the function of variable depth h through three points of $(0, h_0)$, $(l/2, nh_0)$ and (l, h_0) in rectangular coordinates (x, h) is determined as follows:

$$h = h_0\left[-4(n-1)\left(\frac{x}{l}\right)^2 + 4(n-1)\left(\frac{x}{l}\right) + 1\right], \quad 0 \leqslant x \leqslant l. \tag{4}$$

The volume V of parabolic taper can now be calculated by using Eqs. (2) and (4). The result is

$$V = \int_0^l A\,\mathrm{d}x = m \sin\left(\frac{\pi}{m}\right) \cos\left(\frac{\pi}{m}\right)\beta h_0^2 l, \quad \beta = \frac{1}{15}(8n^2 + 4n + 3). \tag{5.1,5.2}$$

For the sinusoidal taper, the function of variable depth h and volume V are determined:

$$h = h_0\left[(n-1)\sin\left(\frac{\pi x}{l}\right) + 1\right], \quad 0 \leqslant x \leqslant l, \tag{6}$$

$$V = \int_0^l A\,\mathrm{d}x = m \sin\left(\frac{\pi}{m}\right) \cos\left(\frac{\pi}{m}\right)\beta h_0^2 l, \quad \beta = \frac{1}{2}(n-1)^2 + \frac{4}{\pi}(n-1) + 1. \tag{7.1,7.2}$$

3. Governing equation

For deriving the differential equation of buckled shape of column, the free vibration problem of column is introduced. Both ends of the column considered herein are supported by clamped or hinged ends.

The partial differential equation governing the free vibration of the column subjected to an axial compressive load P is [13]

$$\frac{\partial^2}{\partial x^2}\left[EI\,\frac{\partial^2 W(x,t)}{\partial x^2}\right] + \rho A\,\frac{\partial^2 W(x,t)}{\partial t^2} + P\,\frac{\partial^2 W(x,t)}{\partial x^2} = 0, \tag{8}$$

where E is Young's modulus, ρ is mass density and $W(x,t)$ is the dynamic displacement.

The column is assumed to be in harmonic motion, or $W(x,t) = w(x)\sin(\omega t)$. Here, ω is the natural frequency, t is time and $w(x)$ is the amplitude, which is a function of x only.

Now, using equation of $W(x,t) = w(x)\sin(\omega t)$ with Eq. (8) gives the ordinary differential equation governing free vibration of the tapered column with an axial compressive load P. The result is

$$EI\,\frac{\mathrm{d}^4 w(x)}{\mathrm{d}x^4} + 2E\,\frac{\mathrm{d}I}{\mathrm{d}x}\,\frac{\mathrm{d}^3 w(x)}{\mathrm{d}x^3} + \left(E\,\frac{\mathrm{d}^2 I}{\mathrm{d}x^2} + P\right)\frac{\mathrm{d}^2 w(x)}{\mathrm{d}x^2} - \rho A\omega^2 w(x) = 0. \tag{9}$$

It is well known that the natural frequency ω decreases as the compressive load P increases and the natural frequency ω vanishes when the compressive load P coincides with the critical loads B_i, where i is the mode number of buckled shape. Once P reaches B_i, the column buckles in (x,w) plane and becomes to be static state. Thus, substituting $\omega = 0$ and $P = B_i$ into Eq. (9) gives the differential equation governing the buckled shape of the column. The result is

$$EI\,\frac{\mathrm{d}^4 w(x)}{\mathrm{d}x^4} + 2E\,\frac{\mathrm{d}I}{\mathrm{d}x}\,\frac{\mathrm{d}^3 w(x)}{\mathrm{d}x^3} + \left(E\,\frac{\mathrm{d}^2 I}{\mathrm{d}x^2} + B_i\right)\frac{\mathrm{d}^2 w(x)}{\mathrm{d}x^2} = 0. \tag{10}$$

To facilitate the numerical studies and to obtain the most general results for this class of problem, the following non-dimensional system variables are introduced:

$$\xi = \frac{x}{l}, \quad \eta = \frac{w}{l}, \quad b_i = \frac{B_i l^2}{\pi^2 E I_e} \tag{11-13}$$

in which ξ and η are normalized by column length l and b_i is the critical load parameter. Also, I_e in Eq. (13) is the moment of inertia of area of cross-section of a uniform column with circular cross-section whose volume is V. Such I_e is determined easily as $I_e = V^2/(4\pi l^2)$.

When Eq. (3) and each of dI/dx and d^2I/dx^2 obtained by differentiating Eq. (3) are substituted into Eq. (10) and the non-dimensional forms of Eqs. (11)–(13) are used, the result is

$$\frac{d^4\eta}{d\xi^4} = a_1 \frac{d^3\eta}{d\xi^3} + (a_2 + a_3 b_i) \frac{d^2\eta}{d\xi^2}. \tag{14}$$

For parabolic tapers, the coefficients a_1-a_3 in Eq. (14) are

$$a_1 = 32(n-1)(2\xi - 1)\frac{1}{j}, \quad a_2 = -32(n-1)^2\left(28\xi^2 - 28\xi + 6 - \frac{1}{n-1}\right)\frac{1}{j^2}, \tag{15.1,15.2}$$

$$a_3 = -\frac{3\pi m \tan(\pi/m)\beta^2}{3 + \tan^2(\pi/m)}\frac{1}{j^4}, \tag{15.3}$$

where

$$j = -4(n-1)\xi^2 + 4(n-1)\xi + 1. \tag{15.4}$$

And for sinusoidal tapers, the coefficients a_1-a_3 in Eq. (14) are

$$a_1 = -8\pi(n-1)\cos(\pi\xi)\frac{1}{j}, \quad a_2 = 4\pi^2(n-1)[\sin(\pi\xi)j - 3(n-1)\cos^2(\pi\xi)]\frac{1}{j^2}, \tag{16.1,16.2}$$

$$a_3 = -\frac{3\pi m \tan(\pi/m)\beta^2}{3 + \tan^2(\pi/m)}\frac{1}{j^4}, \tag{16.3}$$

where

$$j = (n-1)\sin(\pi\xi) + 1. \tag{16.4}$$

For clamped end, the non-dimensional boundary conditions are obtained as follows:

$$\eta = 0, \quad \frac{d\eta}{d\xi} = 0, \tag{17,18}$$

which imply the displacement and rotation are zero.

For hinged end, the non-dimensional boundary conditions are obtained as follows:

$$\eta = 0, \quad \frac{d^2\eta}{d\xi^2} = 0, \tag{19,20}$$

which imply the displacement and bending moment are zero.

4. Numerical examples and discussions

A FORTRAN computer program incorporating the above analysis was written to calculate the critical load parameters b_i for a given column geometry. The numerical methods described by Lee et al. [14], were used to solve the differential equation (14), subjected to the end constraints selected from Eqs. (17), (18) or Eqs. (19), (20). The Runge–Kutta method was used to integrate the differential equations and the determinant search method combined with the Regula–Falsi method was used to determine the eigenvalues of b_i.

Note that once a column buckles due to the first critical load B_1, i.e. buckling load, the higher critical loads B_i ($i = 2, 3, 4\ldots$) only have the mathematical meaning in the real structural system. Therefore, the first critical load parameters b_1, namely buckling load parameters b_1, are only calculated in the numerical examples of this study.

The first numerical study is shown in Table 1 in which b_1 of this study agree quite well with the reference values. These results served to validate the analysis presented herein.

Table 1
Comparisons of results between this study and references

Geometry	This study	References
$n = 2.32$, circular cross-section[a]	$B_1 = 540$ lbs	$B_1 = 550$ lbs [8]
$n = 1.98$, $m = 3$ [b]	$b_1 = 1.572$	$b_1 = 1.574$ [12]
$n = 1.98$, $m = 4$	$b_1 = 1.362$	$b_1 = 1.362$ [12]
$n = 1.98$, $m = 5$	$b_1 = 1.322$	$b_1 = 1.323$ [12]
$n = 1.98$, $m = \infty$	$b_1 = 1.300$	$b_1 = 1.301$ [12]

[a] $m = \infty$, $V = 9\pi/16\,\text{in}^3$, $l = 15.44$ in, $E = 10 \times 10^6$ psi, sinusoidal taper and hinged–hinged end.
[b] Parabolic taper and hinged–hinged end.

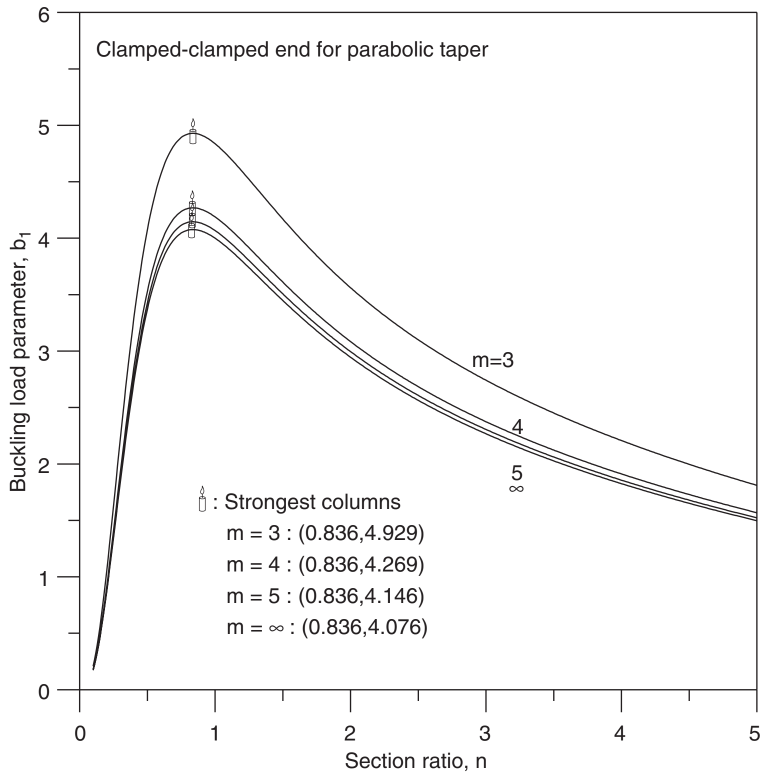

Fig. 2. b_1 versus n curves for parabolic taper with clamped–clamped end.

Shown in Fig. 2 is the variation of b_1 with section ratio n of clamped–clamped end for parabolic taper. All of b_1 with $m = 3, 4, 5$ and ∞ reach the peaks as the section ratio n is increased. The peak point of each curve marked □ represents the strongest column, which shows the largest buckling load parameter for a given set of side number m, taper type and end constraint. For example, the buckling load parameter b_1 and section ratio n of strongest columns for $m = 3$ (triangular cross-section), parabolic taper, and clamped–clamped end are $b_1 = 4.929$ and $n = 0.836$ as shown in the legend.

The section ratios n and buckling load parameters b_1 of the strongest columns for the parabolic and sinusoidal taper by side number m are summarized in Table 2. Compare the result for parabolic taper, $m = 3$, $n = 1.973$, hinged–hinged end and $(b_1)_{\text{critical}} = 1.572$ corresponding to Keller's "optimal" column taper. Keller [3] obtained $(b_1)_{\text{critical}} \approx 1.6$ for the hinged–hinged end. Thus, the parabolic taper with $m = 3$ (triangular cross-section) and $n = 1.973$ obtained herein is almost the optimal column with hinged–hinged end. It is found that

Table 2
Configuration of strongest columns for parabolic and sinusoidal tapers

Taper type	End constraint	m	n	b_1
Parabolic taper	Clamped–clamped end	3	0.836	4.929
		4	0.836	4.269
		5	0.836	4.146
		∞	0.836	4.076
	Clamped–hinged end	3	1.174	2.503
		4	1.174	2.167
		5	1.174	2.105
		∞	1.174	2.070
	Hinged–hinged end	3	1.973	1.572
		4	1.973	1.362
		5	1.973	1.322
		∞	1.973	1.300
Sinusoidal taper	Clamped–clamped end	3	0.854	4.904
		4	0.854	4.247
		5	0.854	4.125
		∞	0.854	4.056
	Clamped–hinged end	3	1.183	2.507
		4	1.183	2.171
		5	1.183	2.108
		∞	1.183	2.073
	Hinged–hinged end	3	1.850	1.558
		4	1.850	1.349
		5	1.850	1.310
		∞	1.850	1.288

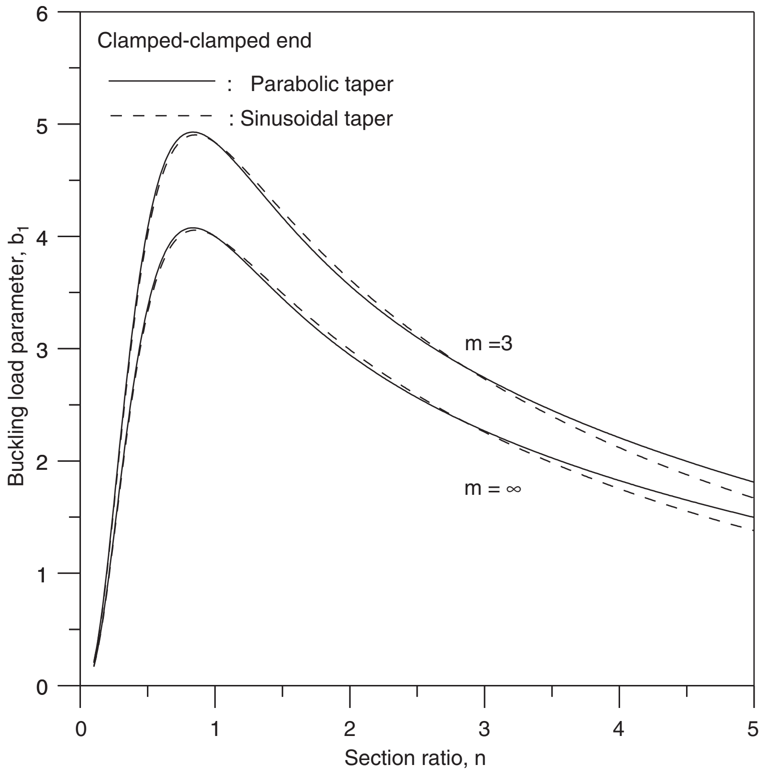

Fig. 3. b_1 versus n curves by taper type with clamped–clamped end.

the section ratios n of strongest columns are the same regardless of side number m when the taper type and end constraint are remaining constant.

The effect of taper type on the buckling load parameter for the clamped–clamped end is presented in Fig. 3. The difference between the solid (parabolic taper) and dashed (sinusoidal taper) curves becomes higher as the section ratio n gets higher value. The difference between two curves for clamped–hinged and hinged–hinged ends, not presented in this paper, becomes more pronounced comparing that of clamped–clamped end.

5. Concluding remarks

The numerical methods developed herein for computing buckling loads of solid tapered columns with regular polygon cross-section and constant volume are found to be especially robust and reliable over a wide and practical range of system parameters. Differential equation governing the buckled shape of column is derived. The parabolic and sinusoidal tapers are chosen as the variation taper. The equation is numerically solved using the Runge–Kutta method and the determinant search method for numerical integration and calculating the eigenvalue, respectively. The numerical results obtained in this study agree quite well with those published in references. According to the variation of non-dimensional system parameters of the columns, the buckling load parameters are reported, and the configurations of strongest columns are also determined.

Acknowledgement

The first author acknowledges the Wonkwang University, Korea for financial support in 2005.

References

[1] J.M. Gere, S.P. Timoshenko, *Mechanics of Materials*, Brooks/Cole Engineering Division, 1984.
[2] R.T. Haftka, Z. Grudal, M.P. Kamat, *Elements of Structural Optimization*, Kluwer Academic Publisher, Dordrecht, 1990.
[3] J.B. Keller, The shape of the strongest column, *Archive for Rational Mechanics and Analysis* 5 (1960) 275–285.
[4] I. Tadjbakhsh, J.B. Keller, Strongest columns and isoperimetric inequalities for eigenvalues, *Journal of Applied Mechanics (ASME)* 29 (1962) 159–164.
[5] J.E. Taylor, The strongest column—an energy approach, *Journal of Applied Mechanics (ASME)* 34 (1967) 486–487.
[6] J.B. Keller, F.I. Niordson, The tallest column, *Journal of Mathematics and Mechanics* 16 (1966) 433–446.
[7] E.F. Masur, Optimal structural design under multiple eigenvalue constraints, *International Journal of Solids and Structures* 20 (1984) 211–231.
[8] J.F. Wilson, D.M. Holloway, S.B. Biggers, Stability experiments on the strongest columns and circular arches, *Experimental Mechanics* 11 (1971) 303–308.
[9] D.C. Barnes, The shape of the strongest column is arbitrarily close to the shape of the weakest column, *Quarterly of Applied Mathematics* 46 (1988) 605–609.
[10] S.J. Cox, M.I. Overton, On the optimal design of columns against buckling, *SIAM Journal on Mathematical Analysis* 23 (1992) 287–325.
[11] T.M. Atanackovic, S.S. Simic, On the optimal shape of a Pflüger column, *European Journal of Mechanics A—Solids* 18 (1999) 903–913.
[12] B.K. Lee, S.J. Oh, Elastica and buckling load of simple tapered columns with constant volume, *International Journal of Solids and Structures* 37 (2000) 2507–2518.
[13] S.P. Timoshenko, D.H. Young, W. Weaver Jr., *Vibration Problems in Engineering*, Wiley, New York, 1974.
[14] B.K. Lee, A.J. Carr, T.E. Lee, D.S. Ahn, Elasticas and buckling loads of shear deformable tapered columns, *International Journal of Structural Stability and Dynamics* 5 (3) (2005) 317–335.